Multi-time measurement and displacement current in time-dependent quantum transport

X.Oriols, F.L.Traversa, G.Albareda, A.Benali, A. Alarcón, S. M. Yaro, X.Cartoixà
Dept. d'Enginyeria Electrònica, Universitat Autònoma de Barcelona (UAB)
E-mail: xavier.oriols@uab.es

***Abstract*—With the aim of manufacturing faster and smaller devices, the electronic industry is today entering into the nanoscale and the high frequency regimes. In this particular scenario, the dynamics of the electron charge becomes affected by quantum mechanical laws, both, for its spatial or temporal description. We have recently shown that Bohmian trajectories allow a direct treatment of the time-dependent many-particle interaction among electrons with an accuracy comparable to Density Functional Theory techniques. In addition, Bohmian mechanics, by combining wave functions and trajectories, provides a very simple description on how to describe multi-time measurements in quantum scenarios. Using the previous formalism, in this work we present a general purpose time-dependent 3D quantum electron transport simulator named BITLLES (Bohmian Interacting Transport in large low-dimensional Electronic Structures) especially indicated for AC, transients and noise predictions. As a numerical example of its capabilities, we compute the full electrical characteristics (DC, High frequency and fluctuations) of a Resonant Tunneling Diode.**

INTRODUCTION

Due to the increase of the complexity and cost of the technological processes necessary to fabricate nanodevice prototypes, physical theories on electron transport constitute at this moment a research and development cost reduction amount up to 40% [1]. A great scientific effort has been devoted to describe DC properties of quantum devices. However, predicting dynamic properties (AC, transient, noise, etc.) of quantum devices is still a very challenging task for the scientific community; mainly because of two reasons. First, a multi-time measurement of the current is needed when computing dynamic properties, which implies discussing the (non-unitary) time-evolution of the quantum device when the current is measured. Second, understanding the time-dependent behavior of electron devices implies dealing with conduction plus displacement currents. The consideration of the displacement current requires, in turn, the time-dependent solution of the many-particle Schrödinger equation. In the next two subsections, we discuss both difficulties in detail.

A. The role of the displacement current

The displacement current is routinely considered in the dynamic simulation of semi classical devices. However, in spite of the explicit efforts done by reputed scientist such as Landauer [2] and Buttiker [3] to publicize the important role of the displacement current in quantum scenarios, it is not always explicitly considered. For this reason, we will repeat here a quite simple exercise emphasizing the relevance of the displacement current [4].

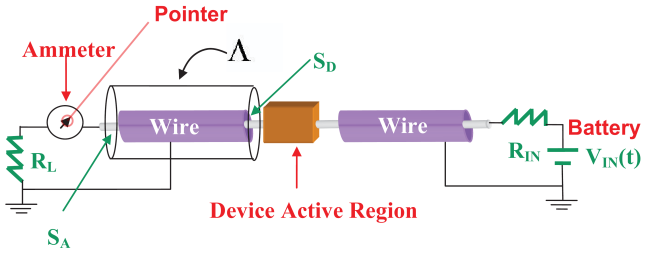

Fig. 1. Schematic representation of the different elements that constitutes any experimental setup. Only the device active region is explicitly considered as the simulating box. The rest of degrees of freedom (associated to the cables, batteries, ammeter, etc) are not explicitly considered in the simulations.

In the scheme of Fig. 1, the device active region constitutes the simulating box. The rest of parts are not explicitly simulated (cables, batteries, ammeter) but they are present in any experimental setup. The experimental current is that measured on the surface S_A. However, only predictions about the current flowing through the surface S_D are computationally accessible. The conduction (particle) current density $\vec{J}_c(\vec{r},t)$ through S_D is not equal to that through S_A. For example, in a two parallel plates capacitor, the number of electrons crossing the surface S_D between the plates is certainly not equal to the number of electrons crossing a surface S_A in the cable. Thus, the conduction (particle) current alone, $\vec{J}_c(\vec{r},t)$, is not what it is measured by the ammeter.

Under the assumption that the cable behaves as a two-terminal element, the current though the surface of the cylindric volume Λ of Fig. 1 parallel to the cable is zero. Then, we are looking for a definition of the total density current, $\vec{J}_T(\vec{r},t)$, that satisfies $\int_{S_\Lambda} \vec{J}_T(\vec{r},t)\ d\vec{s} = 0$ (where S_Λ is the total surface of the cylinder) or its local version $\vec{\nabla}\vec{J}_T(\vec{r},t) = 0$.

To define such current, we consider the continuity equation $d\rho(\vec{r},t)/dt + \vec{\nabla}\vec{J}_c(\vec{r},t)$ and the Gauss equation

$$\vec{\nabla}\vec{E}(\vec{r},t) = \rho(\vec{r},t)/\epsilon, \tag{1}$$

with $\rho(\vec{r},t)$ the charge density of all the particles, ϵ the dielectric constant and $\vec{E}(\vec{r},t)$ the self-consistent electric field. Putting (1) into the continuity equation, we arrive at:

$$\vec{\nabla}\left(\vec{J}_c(\vec{r},t) + \epsilon\frac{d\vec{E}(\vec{r},t)}{dt}\right) = 0, \tag{2}$$

that properly integrated in the appropriate surface gives:

$$I_{S_A}(t) = \int_{S_A} \vec{J}_c(\vec{r},t)d\vec{s} + \int_{S_A} \epsilon \frac{d\vec{E}(\vec{r},t)}{dt} d\vec{s}. \quad (3)$$

The first integral is the conduction current, $I_c(t)$, while the second the displacement current $I_d(t)$. By construction, the sum of the two currents ensures that the measured current $I_{S_A}(t)$ is exactly equal to the simulated $I_{S_D}(t)$, at any time.

It is interesting to notice that the role of the displacement current is much less relevant for DC predictions. The reason is because, the time averaged displacement current becomes zero:

$$\langle I_d(t)\rangle = lim_{T\to\infty} \frac{1}{T}\int_0^T dt \int_{S_A} \epsilon \frac{d\vec{E}(\vec{r},t)}{dt} d\vec{s}$$
$$= lim_{T\to\infty} \int_{S_A} \epsilon \frac{\vec{E}(\vec{r},T) - \vec{E}(\vec{r},0)}{T} d\vec{s} = 0. \quad (4)$$

The average value of the displacement current is zero because the electric field $\vec{E}(\vec{r},T)$ on any surface S does not monotonically grow, but just fluctuates around $\vec{E}(\vec{r},0)$. However, for AC, transients and noise computations, considering the conduction (particle) plus the displacement currents is of fundamental relevance. The explicit consideration of the latter in quantum scenarios needs to include the many-body Coulomb interaction among the electrons. As we will discuss in subsection I-A, the quantum treatment of such many-body problem is not at all simple.

B. The role of the multi-time measurement

Another difficulty appears also when making quantum predictions of the AC, transients and noise properties. This additional difficulty is not present in classical formalisms because the process of measurement has a quite passive role there, while in the orthodox explanation of quantum theory, it has a very fundamental role. In fact, the orthodox (Copenhagen) explanation of the time-evolution of quantum systems follows two laws; one related to the evolution of the wave function without measurement and another with measurement [5].

- The time-evolution of a state $\phi(x,t) = \langle x|\phi(t)\rangle$ without measuring is determined by Hamiltonian operator $\hat{H}$ through the well-known Schrödinger equation:

  $$i\hbar \frac{d}{dt}\langle x|\phi(t)\rangle = \langle x|\hat{H}|\phi(t)\rangle, \quad (5)$$

  that can be rewritten in terms of the time-evolution operator $\hat{U}(\tau)$ as:

  $$|\phi(t)\rangle = e^{-i\frac{\hat{H}\tau}{\hbar}}|\phi(0)\rangle = \hat{U}(\tau)|\phi(0)\rangle. \quad (6)$$

- The time-evolution of a state $\phi(x,t) = \langle x|\phi(t)\rangle$ when measured leads to one of the possible eigenstates $|u_i(t)\rangle$ of the current operator $\hat{I}$. For simplicity, we have considered a measurement process described by a (non-degenerate) projective measurement. Such evolution can be written through the projector:

  $$|\phi(t)\rangle = |u_i(t)\rangle\langle u_i(t)|\phi(0)\rangle. \quad (7)$$

After presenting these two dynamical laws, let us discuss why the second is not fully appreciated when discussing DC quantum transport. Under the reasonable assumption of ergodicity, the DC current can be computed from an ensemble average $\langle I\rangle = \sum_i I_i P(I_i)$. Since the probability of getting the value of the current I_i can be written (following the Born law) as $P(I_i) = |\langle\phi|u_i\rangle|^2 = \langle\phi|u_i\rangle\langle u_i|\phi\rangle$, we get $\langle I\rangle = \sum_i I_i\langle\phi|u_i\rangle\langle u_i|\phi\rangle$. Then, using the definition of projective operator $\hat{I}|u_i\rangle = I_i|u_i\rangle$ and the orthonormal condition, $1 = \sum_i |u_i\rangle\langle u_i|$, we get the final result $\langle\phi|\hat{I}|\phi\rangle$. Therefore, for the computation of the DC quantum current, a single time measurement is enough and only the system state $|\phi\rangle$ and the current operator $\hat{I}$ (not its eigenstates) are needed in the computation.

However, the relevance of expression (7) becomes fully evident when we are interested in discussing multi-time measurements; for example, the noise, i.e. the fluctuations of the current around the average DC value. Such noise is quantified through the use of the autocorrelation function, $R(\tau) = \langle I(t+\tau)I(t)\rangle - I_{DC}^2$ that involves, at least, the measurement of the current at time $t_1 = t$, $I(t_1)$, and time $t_2 = t+\tau$, $I(t_2)$. In particular, the ensemble average value of the product of the current $I(t_2)I(t_1)$ is simply given by:

$$\langle I(t_2)I(t_1)\rangle = \sum_j \sum_i I_j(t_2)I_i(t_1)P(I_j(t_2), I_i(t_1)). \quad (8)$$

The probability $P(I_j(t_2), I_i(t_1))$ can be computed again, from Born law, as the modulus square of the initial state that suffers the following three time-evolutions. First, at time t_1, the system wave function is transformed into one particular eigenstate $|u_i\rangle$ due to the first measurement, $I_i(t_1)$, Eq. (7). Then, from t_1 till t_2, the system evolves according to the Schrödinger equation, Eq. (6). The final sate, after another measurement of $I_j(t_2)$, following Eq. (7), is $|\phi(t_2)\rangle = |u_j\rangle\langle u_j|\hat{U}(\tau)|u_i\rangle\langle u_i|\phi(0)\rangle$. Certainly, the Schrödinger equation alone is not enough to correctly predict such noise properties.

Among other formalisms available to deal with quantum transport, Buttiker [3] was the first to address both problems mentioned above by extending the first quantization proposal of Landauer towards the second quantization language in terms of creating and annihilating operators, allowing a proper treatment of the measurement and (many-body) displacement current. Here we present a quite different quantum transport formalism based on the use of the conditional wave function: a many-particle wave function where some degrees of freedom are substituted by quantum Bohmian trajectories [5]. The formalisms presented here does also perfectly capture the two dynamic aspects discussed above: the need for a many-body approximation to deal with the displacement current and the special treatment of the quantum measurement. Our formalism can be adapted to any realistic situation and we do also develop a quantum transport simulator, named BITLLES (Bohmian Interacting Transport in large low-dimensional Electronic Structures) [6]. Both the formalism and the simulator

will be explained below, showing its capabilities and numerical viability.

I. The BITLLES simulator

As discussed in the introduction, it is computationally unfeasible to account for all the degrees of freedom enclosed in the whole solid-state system (battery, wires, sample,...) drawn in Fig. 1. In practical situations, then, we neglect a large part of the degrees of freedom focusing only on $N(t)$ explicitly simulated electrons. In this regard, since we deal with an open system that exchange energy and electrons with outside, we cannot completely specify the initial $N(t)$-particle wave function inside the simulation box because we do not know with certainty the number of electrons $N(t)$, their energies, their positions, etc. In BITLLES, the adaptation of Bohmian mechanics to electron transport in open systems, leads to a quantum Monte Carlo algorithm where randomness appears precisely because of these uncertainties. In particular, we take into account two statistical ensembles of the initial properties of the electrons within our numerical simulations [5], [7]. First, a *g-distribution* represents the infinite ensemble of all possible distributions in the initial positions of Bohmian particles. Second, an *h-distribution* takes into account the uncertainty in the number of electrons in the active region $N(t)$, the mean energy associated to their wavepackets and the injection times of each electron, etc.

A. The computation of the displacement current through the many-particle Schrödinger equation

It is well-known that the many-particle Schrödinger equation can be only solved for very few degrees of freedom. Thus, in order to provide an accurate description of the electron-electron correlations, quantum transport simulators must consider a reasonable approximation of this many-particle problem. In this regard, BITLLES nourishes from a recently published algorithm that, on the grounds of Bohmian Mechanics, let us solve the many-particle Schrödinger equation in terms of multiple (single-particle) pseudo-Schrödinger equations without loosing the explicit inclusion of the Coulomb and exchange correlations (at a level comparable to the Time Dependent Density Functional Theory) [8]. An introductory review on Bohmian mechanics can be found in [5].

Following reference [8] a many-particle Bohmian trajectory $\vec{r}_a[t]$ associated to an a-electron can be computed from the following single-particle wavefunction, $\Psi_a(\vec{r}_a,t)$, solution of the next single-particle pseudo-Schrödinger equation:

$$i\hbar\frac{\partial\Psi_a(\vec{r}_a,t)}{\partial t} = \{-\frac{\hbar^2}{2m}\nabla^2_{\vec{r}_a} + U_a(\vec{r}_a,\vec{R}_a[t],t) + G_a(\vec{r}_a,\vec{R}_a[t],t) + i\cdot J_a(\vec{r}_a,\vec{R}_a[t],t)\}\Psi_a(\vec{r}_a,t), \quad (9)$$

where we define $\vec{R}_a[t] = \{\vec{r}_1[t],\vec{r}_{a-1}[t],\vec{r}_{a+1}[t],\vec{r}_N[t],t\}$ as a vector that contains all Bohmian trajectories except $\vec{r}_a[t]$. The explicit expression for the potentials $G_a(\vec{r}_a,\vec{R}_a[t],t)$ and $J_a(\vec{r}_a,\vec{R}_a[t],t)$ are in general unknown and need educated guesses [8]. On the contrary, the term $U_a(\vec{r}_a,\vec{R}_a[t],t)$ includes all Coulomb correlations without any approximation [8],[9]. In one hand, $U_a(\vec{r}_a,\vec{R}_a[t],t)$ in Eq. (9) is computed through the following 3D Poisson equation:

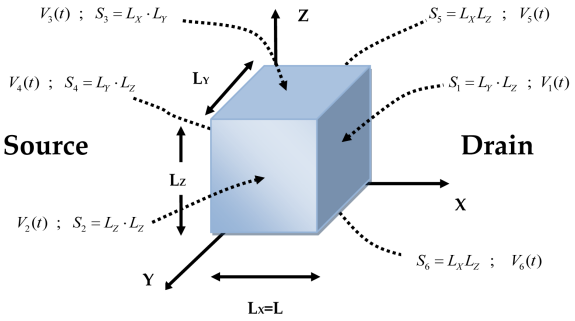

Fig. 2. Volume Ω. Schematic representation of the arbitrary 3D geometry considered in this article as the simulation box for the computation of quantum transport ensuring local current conservation.

$$\nabla^2_{\vec{r}_a}\left(\varepsilon(\vec{r_a})U_a(\vec{r_a},\vec{R}_a[t],t)\right) = \rho_a(\vec{r}_a,\vec{R}_a[t],t), \quad (10)$$

where $\rho_a(\vec{r}_a,\vec{R}_a[t],t)$ is the the charge density associated to all the charged particles in the active region except the a-electron, i.e. we consider a Coulomb potential (or electric field) for each one of the $N(t)$ electrons [9].

It is important to emphasize that the electric field used for the computation of the displacement current mentioned in Sec. -A is computed from expression (1) , while the potential (or electric field) that governs the dynamics of the electrons from expression (10). As mentioned before, such procedure justifies that the total time dependent current computed in a particular surface of the simulating box is equal to that measured by an ammeter, i.e. "current conservation" must be guaranteed [5]. In BITLLES, such a condition is achieved by computing the total (conduction plus displacement) current in a particular volume through an algorithm based on the Ramo-Shockley-Pellegrini theorems [10], [12], [11], [14]. In the Fig. 2, we represent the 6 surfaces of a parallelepiped where the current is computed. (see Fig. 3)

On the other hand, in order to ensure "overall charge neutrality" and "current conservation" in the whole closed circuit, the above $N(t)$ Poisson equations must be accompanied by a rigorous treatment of the active region boundary conditions [15]. In BITLLES, the charge density, the electric field and the scalar potential are all coupled to the injection model by taking into account the electrostatic interaction among the electrons within the active region and those in the leads [15]. Only this way the amount of charge on the whole circuit can be set to zero [15].

The Poisson equations in (10) together with the above described boundary conditions reproduce accurately the electrostatics of the active region. Then, at each simulation time step, dt, the resulting $N(t)$ potential energies are introduced into the $N(t)$ pseudo-Schrödinger equations defined in (9). These overall procedure provides a self-consistent solution of the Poisson and the many-particle Schrödinger equation beyond a mean field level [5], [7], [9], [15], [10].

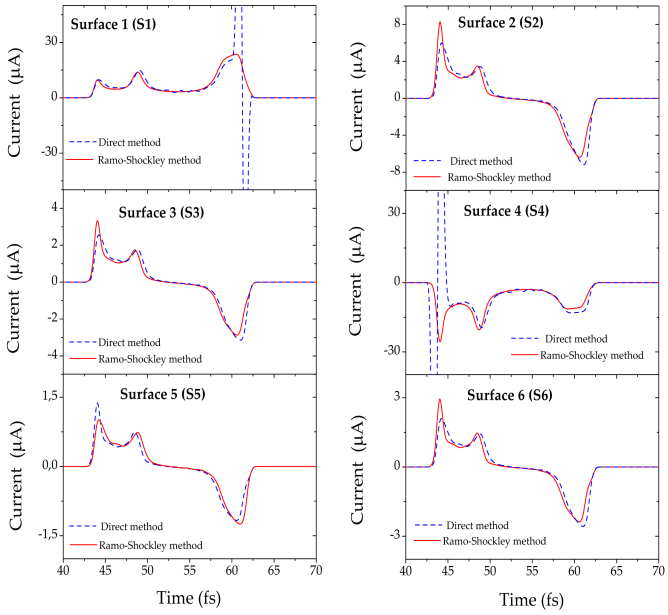

Fig. 3. Time-dependent total current computed on the six surfaces that form the volume Ω of Fig. 2.. The computation of the current within the direct method (dashed lines) has spurious effects that are not present when the Ramo-Shockley-Pellegrini theorem (solid line) is used.

B. The computation of multi-time (measured) currents through Bohmian trajectories

The computational algorithms of the orthodox and Bohmian explanations of a multi-time measurement process are different but, by construction, they both provides identical ensemble results [5]. The differences and similitudes can be easily visualized through the time-evolution of a wave packet impinging upon a tunneling barrier, while being measured during several times. See Fig. 4. The wave packets in Fig. 4 represent the solution of the (unitary) Schrödinger equation for a wave packet incident upon a tunneling barrier, at different times. The initial wave packet (with norm equal to one) is divided into a transmitted plus a reflected wave packet. According to the orthodox (Copenhagen) algorithm, when the system is measured at time t_2, a nonunitary evolution appears in the wave function and, randomly, the reflected wave packet disappears. Only the transmitted wave packet describes the electron at time t_2. Then, when the system is measured again at t_3, the electron is still represented by the transmitted wave packet alone.

Alternatively, the same unitary and nonunitary evolution can be explained by adding a Bohmian trajectory to the previous wave function evolution. The initial position of the Bohmian trajectory is selected randomly at the initial time t_0. Then, at times t_2 and t_3, the evolution of the trajectory is clearly only determined by the transmitted wave packet. The reflected wave packet is an "empty wave" that has no effect on the evolution of the trajectory. As expected, the probability of measuring, first, the particle as being transmitted at time t_1 and measuring, after, the same particle as being reflected at time t_2 is zero either with orthodox or Bohmian mechanics.

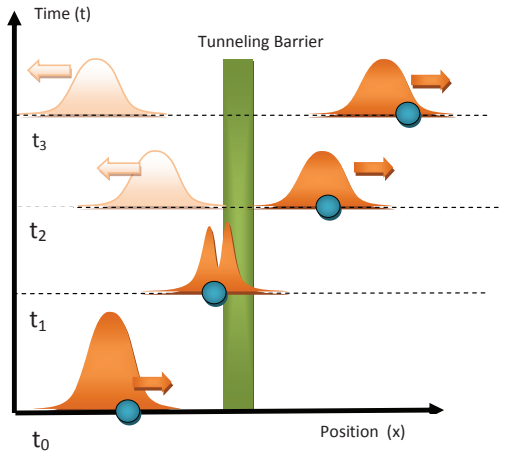

Fig. 4. Schematic representation of a wave packet impinging upon a tunneling barrier, while being measured at times t_1, t_2, t_3 and t_4. The orthodox explanation of the multi-time measurement uses the wave packet alone, the the Bohmian explanation uses the wave packet plus an initially random trajectory. Both explanations are identical.

Here, we have implicitly assumed that the eigenstates of the current operator $\hat{I}$ discussed in Sec -B are transmitted wave packets for positive currents, and reflected ones for negative currents, which corresponds to momentum eigenstates of an operator related to the total momentum operator.

II. Numerical results

In the following subsections, the BITLLES simulator is used to predict the electrical characteristics of an RTD consisting on two highly doped drain-source $GaAs$ regions (the leads), two $AlGaAs$ barriers and a quantum well.

A. Coulomb correlations in DC scenarios

As a first example, we consider the influence of the (many-body) Coulomb correlations even for the DC current-voltage characteristic. Although the displacement current is zero here when time-averaged, the explicit correct consideration of many-body Coulomb effects have effect also on the DC properties.

In Figure 5, we present a comparison between three different current-voltage characteristics: (a) using the many-particle algorithm described in section I (solid circles), (b) neglecting the interaction between the active region and the leads, i.e. using standard Dirichlet external bias boundary conditions (open circles), (c) using these Dirichlet conditions and switching off the Coulomb correlations in the active region (open triangles). As it can be observed, the differences between these three approaches appear not only in the magnitude of the current but also in the position and shape of the resonant region [9], [15].

B. Coulomb correlations in high frequency scenarios

We present the transient current response, $I_{tran}(t)$, when an input step voltage is applied in the negative differential

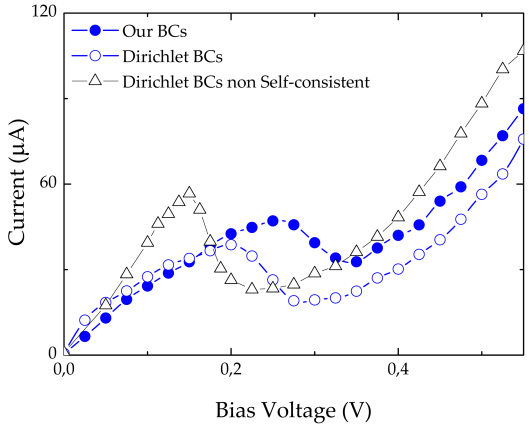

Fig. 5. RTD Current-voltage DC characteristic. Results taking into account the Coulomb correlations between the leads and the active region are presented in solid circles. Open circles refer to the same results neglecting the lead-active region interaction. Open triangles refer to a wholly non-interacting scenario, i.e. both coulomb interaction between the leads and the active region and coulomb interaction among electrons within the active region are neglected.

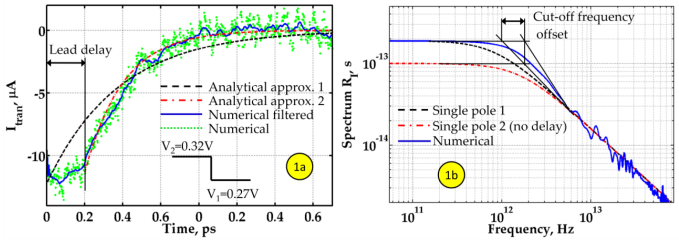

Fig. 6. $I_{tran}(t)$ an its Fourier transform in inset a and b respectively. The **BITLLES** numerical results are compared with analytical RLC circuits.

conductance region (see the inset of Fig. 6). As pointed out in the inset $1a$, $I_{tran}(t)$ manifests a delay of about $0.1ps$ with respect to the step input voltage due to the dynamical response of the electric field in the leads. After this delay, the current response becomes RLC-like (dashed and dashed-dotted analytical lines), i.e. purely exponential. Fourier transforming $I_{tran}(t)$ (inset b) and comparing the result with the single pole spectra (i.e. the Fourier transform of the RLC-like analytical responses represented by dashed and dashed-dotted lines), we are able to estimate the cut-off frequency (about 1.6 THz for this particular device) and the frequency offset (about 0.76 THz) due to the delay [16], [5].

C. Current-current correlations

Finally, we show the ability of BITLLES to compute noise features. We discuss how the many-particle Coulomb correlations affect the Fano factor (i.e. zero frequency noise in units of average current). We investigate the correlation between an electron trapped in a resonant state during a dwell time τ_d and the ones remaining in the left reservoir. This correlation occurs essentially because the trapped electron perturbs the potential energy felt by the electrons in the reservoir. In the limit of non-interacting electrons or mean field approximations, the Fano factor will be essentially proportional to the partition noise. However if the Coulomb correlations are self-consistently

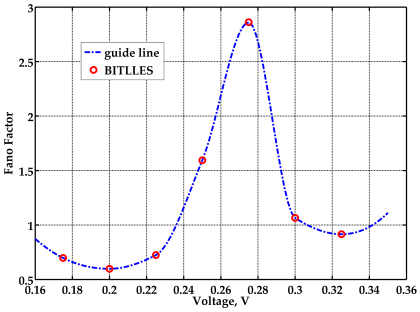

Fig. 7. Fano Factor evaluated as a function of the RTD bias voltage.

included in the simulations, such a result is no longer obtained (see Fig. 7). Roughly speaking, an electron tunneling into the well from the cathode raises the potential energy of the well by an amount of e/C_{eq}, where e is the electron charge and C_{eq} the equivalent capacitance of the structure. As a consequence, the density of states in the well is shifted upwards by the same amount (see Fig. 8) [5].

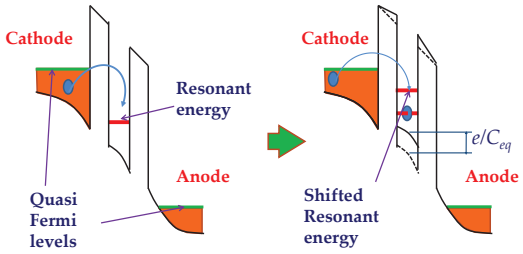

Fig. 8. Schematic representation of the RTD band diagram deformation caused by a particle tunneling through the well.

This phenomenon can affect the noise in the following ways: if the resonant energy E_{R_1} is over the bottom of the conduction band in the emitter, then when an electron enters into the well the density of states inside the well is raised without too much changing the transmittance of the sample. The noise remains in the sub-poissonian regime already present in the limit of partition noise. Contrarily, if the resonant energy is below the conduction band in the emitter, the presence of an electron in the well makes accessible the resonant energy to other electrons staying near the bottom of the emitter conduction band. Therefore, additional electrons in the emitter can tunnel into the well thanks to the first transmitted electron. Under these circumstances, the Coulomb interaction tries to regroup the carriers, showing a super-poissonian noise behavior. Due to our accurate treatment of the many-particle Coulomb correlations, BITLLES captures trivially these and other Coulomb blockade effects.

III. Conclusion

As the size of the electron devices reaches the deep nanoscale regime, electron dynamics are determined by the quantum nature. At these scenarios, the role of the displacement current and the multi-time measurement plays cannot be underestimated when determining AC, transients, noise,etc. In this work we have presented a formalism, based on the use of conditional wave functions with Bohmian trajectories, that is able to capture the role of the previous two mentioned issues [5]. This original formalism has been translated into a versatile time-dependent 3D electron transport simulator named BITLLES [6], capable of capturing many-particle transport phenomena (at a level comparable to the Time Dependent Density Functional Theories). The key point of our novel simulator relies on a recently demonstrated algorithm capable of transforming the many-particle Schrödinger equation of N particles into N single-particle pseudo-Schrödinger equations. BITLLES solves the many-particle Coulomb correlations by means of multiple Poisson equations self-consistently coupled to these N time-dependent single-particle pseudo-Schrödinger equations. Accurate boundary conditions capable of assuring "overall charge neutrality" and "current conservation" in time-dependent scenarios describing nanoelectronic devices are obtained by including the Coulomb correlations between the leads and the active region. In addition, the consideration of the quantum multi-time measurement with wave functions plus Bohmian trajectories allows for a quite simple implementation. The (random) trajectories do themselves select the eigenstate after each measurement. The BITLLES simulator constitute then a general purpose simulator specially attractive to be applied to describe AC, transient and noise features of novel nanoelectronic structures. As an example, we have presented three important electrical characteristics of a RTD: DC, AC and current fluctuations.

Acknowledgment

This work was supported through Spanish MEC project MICINN TEC2009-06986.

References

[1] V. Sverdlov, E. Ungersboek, H. Kpsina, and S. Selberherr, Current transport models for nanoscale semiconductor devices, *Materials Science and Engineering: R* **58**,228 (2008).

[2] R. Landauer, Conductance from transmission: common sense points, Physica Scripta, T42, 100, 1992.

[3] Ya.M. Blanter and M. Buttiker, Shot noise in mesoscopic conductors, Physics Reports, 336(12), 1, 2000.

[4] J. D. Jackson *Classical Electrodynamics, 3rd Ed. John Wiley and Sons* , 1975.

[5] X. Oriols and J. Mompart, *Applied Bohmian Mechanics: From Nanoscale Systems to Cosmology*, Editorial Pan Stanford. See also: arXiv:1206.1084v1 [quant-ph].

[6] http://europe.uab.es/bitlles

[7] G. Albareda, *Classical and Quantum Trajectory-based Approaches to Electron Transport with full Coulomb Correlations*, PhD Thesis (2010).

[8] X. Oriols, Quantum trajectory approach to time dependent transport in mesoscopic systems with electron-electron interactions, *Phys. Rev. Lett*. **98**, 066803, 2007.

[9] G. Albareda, J. Suñé, and X. Oriols, Many-particle hamiltonian for open systems with full coulomb interaction: Application to classical and quantum time-dependent simulations of nanoscale electron devices, *Phys. Rev. B*. **79**, 075315, 2009.

[10] A. Alarcón and X. Oriols, Computation of quantum electron transport with local current conservation using quantum trajectories, *Journal of Statistical Mechanics: Theory and Experiment.* **2009**, P01051, 2009.

[11] X. Oriols, A. Alarcón, and E. Fernández-Díaz, Time dependent quantum current for independent electrons driven under non-periodic conditions, *Phys. Rev. B*. **71**, 245322, 2005.

[12] S. Ramo, Currents induced by electron motion, *Proc. IRE*. **27**, 584, 1939.

[13] W. Shockley, Currents to Conductors Induced by a Moving Point Charge, J. Appl. Phys., 9, 635 ,1938.

[14] B. Pellegrini, Electric charge motion, induced current, energy balance, and noise, *Phys. Rev. B* 34, 5921, 1986.

[15] G. Albareda, H. Lopez, X. Cartoixa, J. J. Suñé, X. Oriols, Time-dependent boundary conditions with lead-sample Coulomb correlations:Application to classical and quantum nanoscale electron device simulators, *Phys. Rev. B* **82**, 085301, 2010.

[16] F.L.Traversa, E.Buccafurri, A.Alarcn,G.Albareda, R.Clerc, F.Calmon, A.Poncet, X.Oriols, Time-Dependent Many-Particle Simulation for Resonant Tunneling Diodes: Interpretation of an Analytical Small-Signal Equivalent Circuit, IEEE Transaction on Electron Devices, 58, 2104, 2011.